Diffuse gliomas exhibit whole brain impaired cerebrovascular reactivity

Fierstra, Jorn ; van Niftrik, Christiaan ; Piccirelli, Marco ; Bozinov, Oliver ; Pangalu, Athina ; Krayenbühl, Niklaus ; Valavanis, Antonios ; Weller, Michael ; Regli, Luca

DOI: https://doi.org/10.1016/j.mri.2017.09.017

Originally published at:
Fierstra, Jorn; van Niftrik, Christiaan; Piccirelli, Marco; Bozinov, Oliver; Pangalu, Athina; Krayenbühl, Niklaus; Valavanis, Antonios; Weller, Michael; Regli, Luca (2017). Diffuse gliomas exhibit whole brain impaired cerebrovascular reactivity. Magnetic Resonance Imaging, 45:78-83.
DOI: https://doi.org/10.1016/j.mri.2017.09.017

Elsevier Editorial System(tm) for Magnetic Resonance Imaging

Manuscript Draft

Manuscript Number: MRI-D-17-00345R1

Title: Diffuse gliomas exhibit whole brain impaired cerebrovascular reactivity

Article Type: Original Contribution

Keywords: fMRI, BOLD, diffuse glioma, cerebrovascular reactivity, carbon dioxide

Corresponding Author: Dr. Jorn Fierstra, MD PhD

Corresponding Author's Institution: University Hospital Zurich, University of Zurich

First Author: Jorn Fierstra, MD, PhD

Order of Authors: Jorn Fierstra, MD, PhD; Christiaan H Van Niftrik, MD; Marco Piccirelli, PhD; Oliver Bozinov, MD; Athina Pangalu, MD; Niklaus Krayenbühl, MD; Antonios Valavanis, MD; Michael Weller, MD; Luca Regli, MD

Cover Letter

Zurich, September 25th 2017

Dear Editor,

With great pleasure we send you our revised version of the manuscript with title: "Malignant gliomas exhibit impaired cerebrovascular reactivity" for consideration in Magnetic Resonance Imaging.

We have answered the reviewers comments to the best of our knowledge and on a point-by-point basis.

Please do not hesitate to contact us if you require additional information.

On behalf of all co-authors,

Sincerely,

Jorn Fierstra, MD PhD

Department of Neurosurgery, University Hospital Zurich
Frauenklinikstrasse 10
8091 Zurich, Switzerland
Phone: +41-44-2551111
Fax: +41-44-2554505
E-mail: jorn.fierstra@usz.ch

Response to Reviewers' comments

1. **P5, section 2.2: CO2 stimuli are often longer and have multiple blocks. Could you comment on the reasons why a shorter duration scan with a single CO2 block was used here?**

   Answer:
   Due to the nature of the RespirAct, which allows for a reproducible, standardized CO2 stimulus, similar among all subjects, we aimed for a short duration of CO2 application (ca. 80 seconds), which would still allow for a significant BOLD signal change. This approach combines good results with better CO2 tolerability by the subjects, due to the shorter CO2 application time (within the physiological range).

2. **P5, section 2.3: Can you comment on the reasons for applying both low pass filtering and the Loess temporal smoothing? Presumably the latter is removing low frequency drift, leaving a narrow passband. Is there a risk you are filtering out true CO2 stimulus related signal? A simple high pass filter only would give me more confidence that this wasn't the case.**

   Answer:
   It might be, but the high frequency noise will overrun the hypothetical small BOLD signal fluctuations when using the high pass filter.
   However, the applied CO2 stimulus is mostly in the low frequency range.
   The interesting part, though, is that the prolonged BOLD signal change is better detectable with the robust CO2 stimulus we apply with this novel CO2 technique.

3. **P6, section 2.4: Did you apply the same temporal filtering (low pass +Loess) to the PetCO2 regressor used to fit the data? Sharp transitions in the BOLD data will be lost to the low pass filter, so a better match to the regressor will be possible if it similarly filtered.**

   Answer:
   We obtained the single PetCO2 end-tidal values directly from the RespirAct. We do not subtract the entire CO2 curve. Therefore, this was already a smoothed indication from the real trace. As was shown by Slessarev et al [REF], this end tidal tracing reflects the arterial partial pressure of CO2 very well. Therefore, we did not apply an extra smoothing to PetCO2 tracing.

4. **P6, section 2.4: Could you provide a bit more detail on the process to determine the "optimal delay" of the regressor with respect to the BOLD data? Were any limits imposed on the values that this delay could take and were the resulting maps of delay smoothly varying as expected?**

   Answer:
   Here, we have to redirect the reviewer to our previous paper describing this method in detail (van Niftrik, Piccirelli et al 2017). In this particular manuscript we present a new method to calculate delay based on the signal changes induced by the BOLD signal itself. We direct the method away from a general delay or a delay calculated with a maximum correlation. Therefore, the start of the CO2 Bolus coincides with the

start of the BOLD signal changes (positive or negative). For this method, we did not apply ranges to our delay calculations.

Changes made to the manuscript: Page 6 section 2.4
More details are provided in a previous publication by our group. (16)

5. **P12, section 4.2: Dampening of the BOLD response was briefly mentioned. Since BOLD weighted imaging was used to map CVR this is a point that deserves further attention. It's true that CO2 elevation of ICP could reduce the dynamic range of the BOLD response. However, other global changes could explain the differences observed between patients and controls. The dynamic range of the BOLD response is largely determined by the product of venous CBV, oxygen extraction fraction (OEF) and haematocrit. Of these, it seems most likely that OEF could be disturbed globally in patients, in this case a reduction in OEF. This could be caused by either lower oxygen metabolism or increased CBF and could be investigated using techniques such as TRUST and ASL, respectively, in future work.**

Answer:
Here, we agree with the reviewer that the BOLD signal is dependent of many different variables. However, we must mention that a large part of the BOLD signal is not just influenced by OEF, CBV or Hematocrit, but also by CBF changes induced by the remaining vasodilatory capacity, especially as we use a prospective end tidal gas blender, like the RespirAct.
With a known increased intralesional OEF, the intratumoral CVR should in theory be increased as the potential wash-out of deoxyhemoglobin intralesionally is increased. However, we find a reduced CVR also intralesional. This makes us believe that the vasodilatory capacity (CVR), either through maximal vasodilatation of pre-existing vessels or the formation of new vessels - neoangiogenesis – without the capacity of vasodilation, has a much larger effect on the BOLD signal intralesional.
With respect to the global CVR, it is unknown exactly know to what extent all the factors influence the BOLD signal. It could be related to a reduction in OEF. That is a very exciting research avenue to investigate with either BOLD or other functional imaging techniques as mentioned by the reviewer, like ASL and TRUST.

Changes made to the manuscript: Page 11
Subsequently, with a known increased intralesional Oxygen Extraction Fraction, intralesional CVR should theoretically be higher as compared to the whole brain CVR, as there should be a higher deoxyhemoglobin content present. With an adequate vasodilatory response to a vasodilatory stimulus, the potential wash-out of deoxyhemoglobin is increased leading to a higher CVR. However, our findings show a more severely impaired intralesional CVR, which makes us believe that the vasodilatory capacity has a much larger effect on the BOLD signal intralesional. Ideally a multimodal MR imaging protocol, including OEF and CBF measurements, might better explain the underlying pathophysiology.

Typos

P2, first paragraph: Is there a word missing in the opening sentence: "Cerebral diffuse exhibit perilesional…"

Answer: We have added the word “gliomas” here. This had been erased accidentally.

P5, section 2.2: "build" -> "built"

Answer: This has been changed accordingly.

P7, section 2.6: Last sentence of first paragraph missing full stop.

Answer: corrected accordingly

P11, last paragraph: broken sentence "…whole brain CVR were resp. more and equally impaired…"
Answer: We have revised the sentence.

Title: Diffuse gliomas exhibit whole brain impaired cerebrovascular reactivity

Running Title: Diffuse gliomas exhibit impaired CVR

Authors: Jorn Fierstra, MD PhD[1]; Christiaan van Niftrik, MD[1]; Marco Piccirelli, PhD[2]; Oliver Bozinov, MD[1]; Athina Pangalu, MD[2]; Niklaus Krayenbühl, MD[1]; Antonios Valavanis, MD[2]; Michael Weller, MD[3]; Luca Regli MD[1]

Affiliations: Departments of Neurosurgery[1], Neuroradiology[2], and Neurology[3], Clinical Neuroscience Center, University Hospital Zurich, University of Zurich, Switzerland

Corresponding author

Jorn Fierstra, MD PhD

Department of Neurosurgery, University Hospital Zurich

Frauenklinikstrasse 10, 8091 Zurich, Switzerland

Phone: +41-44-2551111, Fax: +41-44-2554505 E-mail: jorn.fierstra@usz.ch

Keywords: fMRI, BOLD, diffuse glioma, cerebrovascular reactivity, carbon dioxide

Abstract

Purpose: Cerebral diffuse gliomas exhibit perilesional impaired cerebrovascular reactivity (CVR), yet the degree of impairment as well as its full spatial extent in the brain remains unknown. With quantitative fMRI, we studied twelve subjects with untreated brain diffuse glioma and twelve healthy controls to assess CVR impairment and determine its distribution throughout the brain.

Methods: In a prospective case-control study, quantitative CVR measurements were derived from BOLD fMRI volumes during standardized iso-oxic changes in carbon dioxide. Whole brain CVR was assessed with additional detailed analyses using specific tumor and tissue masks and compared to datasets of healthy controls.

Results: Whole brain CVR was significantly impaired compared to healthy controls (0.11±0.10 versus 0.28±0.8, $p<0.01$). All diffuse glioma patients exhibited even more severely impaired intralesional CVR (mean 0.01±0.06). Increasing tumor volume significantly correlated with severity of intralesional CVR impairment ($p<0.05$, $R^2 = 0.38$), and whole brain CVR impairment ($p<0.05$, $R^2= 0.55$).

Conclusion: Patients with brain diffuse glioma exhibit intralesional and whole brain impaired CVR with severity correlating to tumor volume. Quantitative fMRI may be entertained to study antitumor therapy efficacy by tracking CVR changes and may have a complementary role to better interpret BOLD associated neurovascular uncoupling.

1. Introduction

Neuroimaging plays a pivotal role in treatment response evaluation of brain diffuse gliomas, but is currently limited in accurate depiction of tumor morphology and pathophysiology. (1) (2) For instance, contrast enhanced T1-weighted Magnetic Resonance Imaging (CE-MRI) is imperfect in identifying true tumor tissue due to heterogeneous contrast enhancement, (3) and cannot assess functional parameters such as tumor hemodynamics and molecular characteristics. O-(2-[18F]fluoroethyl)-L tyrosine Positron Emission Tomography (FET-PET) may potentially provide the best functional imaging information, but heterogeneity in (peri)tumor metabolism and long acquisition times may limit clinical applicability. (4) This indicates that the complex molecular biology and pathophysiology of brain diffuse glioma significantly challenges imaging reliability.

From a hemodynamic perspective, diffuse gliomas are believed to disrupt perivascular organization due to co-option of tumor cells accumulating around existing vasculature. (5) As a result the blood vessel walls are destabilized with decreased pericyte coverage, cells thought to be involved in blood flow autoregulation, (6) leading to inability of viable neurons to enhance regional cerebral blood flow (termed `neurovascular uncoupling`) (7-10) a phenomenon that may be more pronounced with increasing tumor volume. (11) Assessing these alterations of cerebrovascular autoregulation with Blood Oxygen-Level Dependent (BOLD) functional (f)MRI cerebrovascular reactivity (CVR) may therefore better depict glioma tissue and locate areas of neurovascular uncoupling and tumor-induced neuroplasticity, ie. healthy brain tissue with `silenced` viable neurons.(7-9,12) This may otherwise manifest itself as false negative activation on conventional task-based BOLD fMRI. Our aim therefore was to elaborate on these encouraging first results by others by further studying the severity of CVR impairment and its distribution throughout the brain.

We prospectively enrolled twelve consecutive subjects harboring untreated brain diffuse glioma, and hypothesized that these patients exhibit widespread impaired CVR extending the contrast enhancing glioma lesion on T1-weighted MRI. Quantitative CVR was derived from a novel standardized BOLD fMRI + CO_2 examination (13,14) and compared to matched healthy controls undergoing the same protocol. In this study, CVR impairment was present over the entire brain in subjects with diffuse glioma.

2. Methods

The study was approved by the cantonal ethics board of the Canton of Zurich, Switzerland (research protocol KEK-ZH-Nr. 2012-0427). Twelve consecutive subjects with newly diagnosed and untreated brain diffuse glioma (defined as either WHO Grade III or Grade IV as confirmed by histopathological diagnosis) as well as twelve age and sex matched healthy controls were prospectively enrolled. Exclusion criteria were the presence of severe cardiopulmonary disease, standard MRI contraindications, age<18 years old, or the inability or refusal to sign informed consent. Furthermore, healthy controls were screened for no medication use, no medical history of neurological disease.

2.1 MRI protocol

Studies were acquired on a 3 Tesla Skyra VD13 (Siemens, Erlangen, Germany) using a 32-channel head coil with the following parameters: an axial 2D EPI BOLD fMRI sequence planned on the ACPC line plus 20° on a sagittal image with voxel size: 3×3×3 mm^3, acquisition of matrix 64x64x35 slices with ascending interleaved acquisition, slice gap 0.3 mm, GRAPPA factor 2 with 32 ref. lines, Repetition Time (TR)/TE 2000/30 ms, flip angle 85°, bandwidth 2368 Hz/Px, Field of View 192x192 mm^2. Secondly, a high resolution 3D T1-weighted anatomical image was acquired with the same orientation as the fMRI scan for co-registration and overlay purposes. The acquisition parameters were: voxel size: 0.8×0.8×1.0

mm^3 with a Field of View 230x230 mm^2 and resolution of 288x288. 176 slices per slab with a thickness of 1 mm, TR/TE 2200/5.14 ms, TI 900 ms, flip angle 8°. The FLAIR images were acquired with the same orientation as the BOLD and T1-weighted images. The acquisition parameters were as followed 0.9x0.9x1.0 mm^3 with a Field of View 230x230 mm^2 and resolution of 256x256, 176 slices per slab with a thickness of 1 mm, TR/TE 4000/387 ms, TI 1800 ms.

2.2 Standardized iso-oxic CO_2 stimulus

All subjects were asked to refrain from caffeine at least 6 hours before scanning. With the use of a custom built computer controlled gas blender (RepirAct™, Thornhill Research Institute, Toronto, Canada) using the prospective gas targeting algorithms of Slessarev et al. (15), to precisely control partial pressure of end-tidal O_2 ($P_{ET}O_2$) and CO_2 ($P_{ET}CO_2$). Specific improvements and novelties of this technique as compared to other vasoactive stimuli have been described in greater detail previously. (13) BOLD signal changes were induced by a single hypercapnia pseudo square wave. The pseudo square wave consisted of a hypercapnia plateau of 50 mmHg CO_2 for 80 seconds following a 100 seconds baseline of 40 mmHg CO_2. Thereafter, a second baseline of 40 mmHg was maintained for another 100 seconds. During the entire protocol iso-oxia (PO_2 100 mmHg) was maintained.

2.3 Data analysis of BOLD fMRI and T1-weighted image

All images were preprocessed using Statistical Parameter Mapping software (SPM 12, Wellcome Trust Centre for Neuroimaging, Institute of Neurology, University College London; http://www.fil.ion.ucl.ac.uk/spm/). Slice timing correction was applied to correct for the interleaved acquisition. The intra fMRI motion was determined and taken out by realigning the BOLD images to a mean BOLD volume. Subjects with more than 4mm motion were discarded. The T1-weighted image was linearly registered to the mean BOLD volume

for optimal alignment. Automated segmentation of the T1-weighted image yielded grey and white matter, cerebrospinal fluid, skull and skin probability maps. The BOLD images were spatially smoothed with an 8x8x8-mm^3 full width half maximum Gaussian kernel. Temporal smoothing included a low pass filter of 0.125Hz and robust Loess smoothing (dynamic local regression of 6%).

2.4 Cerebrovascular reactivity maps

MRI volumes were analyzed using MATLAB2013 based (The MathWorks, Inc., Natick, United States; (www.matworks.com) in-house written scripts. We determined the optimal delay on a voxel-wise basis by applying an iterative analysis to the data to determine the correct voxel-wise temporal $P_{ET}CO_2$ shift to match the start of the hypercapnia induced BOLD signal change. The shifted $P_{ET}CO_2$ time series was regressed using a linear least square fitting to the BOLD time series on a voxel-per-voxel basis. More details are provided in a previous publication by our group. (16) CVR was defined as the %BOLD signal change per mmHg CO_2. CVR was color-coded between -0.6 and 0.6 and overlaid on the T1 weighted image. Only voxels passing a combined grey and white matter probability of 0.9 were included for overlay and further analysis (Figure 1). Hemispheres were manually segmented in left and right hemisphere and CVR was calculated separately for both.

2.5 Tumor and edema mask determination

The tumor mask was determined by a senior staff neuroradiologist (A.P.). Here, the mask was determined from a contrast enhanced T1-weighted anatomical volume where the contrast-enhancing lesion was depicted. This mask was used to determine intralesional CVR and tumor volume. Intralesional CVR was calculated by projecting the tumor mask on the CVR map (Figure 1). This tumor mask was also mirrored onto the 'unaffected' contralateral hemisphere (excluding the gliomas with a "butterfly" configuration, n= 8) for subsequent

CVR comparison. Regarding this mask only voxels within the grey and white matter were considered for further analysis. Extent of edema was determined and masked using a high resolution FLAIR T2 weighted image. Tumor volume was based on MR voxel proportions and number of voxels within the tumor and calculated in mm^3.

2.6 Statistical Analysis

Continuous variables are presented as mean ± standard deviation. Demographic data and CVR were compared between two groups (diffuse glioma patients versus healthy controls) using independent sample t-tests and Fisher's Exact test [$p<0.05$ was considered significant; $t(24) = 2.064$]. Comparison between the ipsilateral and contralateral tumor masks were done using a paired sample T Test.

As a sub-analysis mean CVR of subjects with grade III and grade IV were compared. Comparisons between groups were done using the Chi-square test or the Fisher's exact test, where appropriate. To corroborate the results of bivariate testing, we constructed a generalized linear model with tumor volume as the independent variable.

3. Results

3.1 Potential confounders affecting CVR measurements in the study cohort

We assessed several comorbidities that could potentially affect CVR findings, such as diabetes, smoking, chronic obstructive pulmonary disease, asthma, hypercholesteremia and hypertension. These did not reveal significant differences in CVR readings between patients with diffuse glioma and healthy controls ($p= 0.45$). Furthermore, since target $P_{ET}CO_2$ and $P_{ET}O_2$ were controlled no significant differences between patients and controls were found for baseline conditions (40.3±1.3 versus 40.5±1.3, $p= 0.55$, respectively), hypercapnia (50 ± 1.4

versus 48.2±1.2, p= 0.43 respectively) and CO_2 step change (p= 0.48). End tidal PCO_2 ($P_{ET}CO_2$) and PO_2 ($P_{ET}O_2$) values for patients are shown in Table 1.

3.2 CVR findings in patients with diffuse glioma and healthy references

To examine whether diffuse glioma impacts cerebrovascular reactivity, we analyzed CVR maps of 12 patients with diffuse glioma (mean age 50 years, range 27-81; 4 females) and compared these to CVR maps of 12 age and sex matched healthy controls. More detailed patient and tumor characteristics are shown in Table 1. Differences in CVR were calculated as the percent change in BOLD signal per mmHg change in $P_{ET}CO_2$ (see Methods section). Whole brain CVR of diffuse glioma patients was significantly impaired compared to healthy controls (0.11±0.10 versus 0.28±0.8, p<0.01; Figure 2 & Table 2). Additionally, individual CVR measurements of both hemispheres, ipsi- and contralateral, were also significantly impaired as opposed to healthy controls (p<0.05). This suggests that diffuse glioma impacts CVR on a widespread scale.

3.3 CVR findings in patients with diffuse glioma

Further detailed analyses were done on diffuse glioma patients. Ipsilateral CVR was significantly more impaired as compared to contralateral CVR (0.10±0.9 vs 0.13±0.9, p<0.01). All diffuse glioma patients exhibited intralesional impaired CVR with an overall mean of 0.01±0.06, which was significantly decreased as compared to whole brain CVR (p<0.05). By flipping the tumor mask onto the contralateral hemisphere, a mirror CVR comparison was done (0.07±0.06) which confirmed a significant impaired CVR within the tumor (p<0.05).

Perifocal edema was determined from a T2-FLAIR volume (see methods) and subsequently analyzed for CVR. This also demonstrated impaired CVR (0.04±0.05), however intralesional CVR was again more impaired (p<0.05). A trend in correlation was observed towards more

severe intralesional and whole brain CVR impairment in WHO grade IV gliomas (grade III (n= 6) versus grade IV (n= 6); 0.12±0.13 vs 0.10±0.07 p=0.77 for whole brain CVR; 0.0±0.06 vs 0.03±0.06 p =0.42 for intralesional CVR). Tumor volume was not a confounder in this analysis. This may actually reach statistical significance in a future, larger series of patients. The significantly impaired CVR findings in patients with diffuse glioma are plotted in Figure 3 for visual appreciation, against a reference CVR value derived from the cohort of healthy subjects. In the supplementary files we have added a movie of whole brain CVR in 1) a healthy subject (Supporting Video S1) and 1) a patient with a diffuse glioma (Supporting Video S2).

3.4 Correlation of CVR impairment versus tumor volume

Since all diffuse glioma patients exhibited whole brain and intralesional CVR impairment, for our final analysis, we determined the association of tumor volume with degree of CVR impairment. Here, severity of intralesional CVR impairment was significantly correlated to tumor volume ($p<0.05$, $R^2 = 0.38$, Figure 4). This correlation was even stronger between whole brain CVR and tumor volume ($p<0.05$, $R^2= 0.55$, Figure 4).

4. Discussion

Quantitative CVR obtained with standardized BOLD fMRI + CO_2 highlights extensive impairment in brain diffuse glioma. All 12 glioma patients exhibited whole brain impaired CVR, and to a greater extent intralesional impaired CVR. Interestingly, a trend was observed towards more severe CVR impairment in glioblastoma (WHO grade IV) patients.

Important to mention is that our data confirm previous findings of intralesional CVR impairment, (7,8,12,17) and that we newly demonstrate presence of CVR impairment in the entire brain with severity correlating to tumor volume. This global presence of impaired CVR

warrants current findings of BOLD fMRI associated perilesional neurovascular uncoupling and tumor-induced neuroplasticity in cerebral diffuse gliomas. Pillai et al. (18,19) have already advocated the importance of a complementary BOLD CVR examination to validate perilesional neurovascular uncoupling, ie. to correct for false negative activation on conventional task-based fMRI. Furthermore, even though the presence of tumor-induced neuroplasticity has univocally been proven by itself, detecting such with BOLD fMRI may have to be interpreted with caution as presence of CVR impairment may also lead to false negative BOLD signal changes. For instance, Southwell et al. (20) measured "less functional reorganization" in patients with larger volume diffuse gliomas. Following this observation Wang et al. (11) have shown that neurovascular uncoupling is more pronounced with increasing tumor volume. Both observations confirm that caution must be taken to interpret these data as increasing CVR impairment may partially influence the readout. Furthermore, these effects may not be limited solely to the perilesional tissue and our current findings underscore the importance of obtaining a quantitative CVR map of the entire brain in order to better validate the presence of BOLD associated neurovascular uncoupling and tumor induced neuroplasticity.

The exact pathophysiological mechanisms causing this vascular dysregulation appear to be complex and remain to be further elucidated. Animal studies in diffuse glioma have indicated smooth muscle vascular tone disruption due to displacement of astrocyte end-feet covering the vascular surface, ie. tumor cell co-option. (5) As a result the blood vessel walls are destabilized with decreased pericyte coverage, cells thought to be involved in CBF autoregulation, (6) leading to inability of viable neurons to enhance regional blood flow. This vascular dysregulation can be a reason for impaired CVR due to altered autoregulation. A second reason may be abnormal neoangiogenesis following increased tumor metabolism, which often results in angioarchitecture lacking smooth muscle cells and vessels therefore are

not able to respond appropriately to a CO_2 stimulus. (21) In this instance, surrounding healthy tissue can still vasodilate (ie. drop vascular resistance) and will redirect blood flow away from the non-responsive abnormal vessels. Indeed, clinical studies have found that a CO_2 stimulus results in redistribution of cerebral blood flow (CBF) from a tumor region with abnormal angiogenesis to a responsive tumor region and surrounding normal tissue, causing a focal steal phenomenon (ie. severely impaired CVR). (12) In contrast, steal phenomenon has not been found in patients harboring low grade gliomas.(12,22) Finally, locally impaired CVR may also be related to mass effect of the tumor on surrounding healthy tissue. The resulting perifocal pressure may alter cerebrovascular autoregulation. Sharma et al. (23) found that CVR impairment was associated with tumor size and midline shift >5mm. Although none of our subjects exhibited acute clinical signs of raised intracranial pressure, mass effect may have indeed contributed to a decreased BOLD signal. This pressure effect can involve the entire brain with increasing tumor volume. In larger tumors, CBF recruitment may exceed the capacity of CVR of the perilesional tissue and therefore impact on the entire brain. The presence of whole brain impaired CVR for such lesions indicates adjustment of healthy blood vessels, ie. dropping vascular resistance in order to compete for adequate blood flow supply. Subsequently, with a known increased intralesional Oxygen Extraction Fraction (OEF), intralesional CVR should theoretically be higher as compared to the whole brain CVR, as there should be a higher deoxyhemoglobin content present. With an adequate vasodilatory response to a vasodilatory stimulus, the potential wash-out of deoxyhemoglobin is increased leading to a higher CVR. However, our findings show a more severely impaired intralesional CVR, which makes us believe that the vasodilatory capacity has a much larger effect on the BOLD signal intralesional.

Ideally a multimodal MR imaging protocol, including OEF and CBF measurements, might better explain the underlying pathophysiology.

Lastly, impaired CVR was also found within the perifocal edema. A report by Ludemann et al. (22) showed that the presence of perifocal edema does not influence CVR measurements obtained with BOLD fMRI, but this finding was based on a small cohort and has not been reproduced. Although we believe that edema may have contributed to perilesional CVR impairment, the fact that intralesional CVR was more severely impaired as compared to whole brain CVR shows that this effect may not be significant. The true influence of edema on perilesional CVR will have to be further studied with more detailed analyses.

4.1 Obtaining CVR measurements

The major challenge for quantifying CVR is the inherent limitation of applying a standardized (vaso)active stimulus in order to reliably and sensitively detect CVR abnormalities. (13) Most studies therefore determine breath-hold based CVR to assess impaired (peri-)lesional CVR by comparing CVR values to the assumingly healthy contralateral hemisphere. (7,12,21,22,24,25) Our data, however, demonstrate that quantitative CVR measurements also reveal substantially impaired CVR in the contralateral hemisphere. A finding that has been confirmed recently by Sam et al. (26) using the same technique. Therefore, breath-hold based CVR calculations may lead to type II statistical error.

For over ten years, we have been successfully employing standardized prospective CO_2 targeting for our BOLD related CVR studies (27,28) and have implemented the same protocol for this study with improved methodological CVR analysis. (16) This has resulted in a quantitative and sensitive (voxel-wise) whole brain CVR analysis in patients with diffuse gliomas. The use of a `healthy` contralateral hemisphere or ROI may also be argued based on these data, since all of our subjects exhibited impaired CVR contralaterally. Although a relative CVR difference may be calculated from a contralateral hemisphere or ROI, using the term healthy may be erroneous. A comparison against a statistical control atlas containing

data of healthy volunteers may therefore provide a more sensitive and reliable quantitative measure to assess the degree of CVR impairment. (29)

4.2 Limitations

Theoretically, impaired CVR may have been the consequence of a `dampened` BOLD response by CO_2 elevations or raised intracranial pressure (ICP) as a result of tumor mass including perifocal edema. (23,30) Although the CVR findings appear to discriminate between patients with diffuse glioma and healthy controls, possible confounders such as co-morbidities and glioma characteristics, might have influenced CVR readings. Even though these features did not demonstrate a statistically significant effect, these analyses are underpowered to reveal possible statistical differences in our cohort, with a relatively small sample size of 24 subjects. In addition, the effect of age, pulmonary disease and history of chronic cigarette smoking, which may ordinarily increase the arterial to end-tidal gradient in spontaneously breathing subjects, might influence CVR readings. However, Ito et al. (31) have argued that, with computer controlled prospective end-tidal targeting, the gradient will nevertheless, be small, even in the presence of lung disease, over a large range of induced PCO_2 and O_2 pressure.

5. Conclusion

Patients with brain diffuse glioma exhibit intralesional and whole brain impaired CVR with severity correlating to tumor volume. A quantitative whole brain CVR evaluation may have a complementary role to better assess BOLD associated neurovascular uncoupling.

Acknowledgments

We would like to express our gratitude to the Neuro-MRI team of the University Hospital Zurich for their support and coordination. None of the authors report conflicts of interest or

will gain financially from this manuscript. This work was supported with the University of Zurich `Filling-the-Gap 2015` and `Forschungskredit: Postdoc 2016` initiative.

6. Reference list

1. Wen PY, Kesari S. Malignant gliomas in adults. N Engl J Med 2008;359(5):492-507.
2. Huang RY, Neagu MR, Reardon DA, Wen PY. Pitfalls in the neuroimaging of glioblastoma in the era of antiangiogenic and immuno/targeted therapy - detecting illusive disease, defining response. Front Neurol 2015;6:33.
3. Chung C, Metser U, Menard C. Advances in Magnetic Resonance Imaging and Positron Emission Tomography Imaging for Grading and Molecular Characterization of Glioma. Semin Radiat Oncol 2015;25(3):164-171.
4. Albert NL, Weller M, Suchorska B, Galldiks N, Soffietti R, Kim MM, la Fougere C, Pope W, Law I, Arbizu J, Chamberlain MC, Vogelbaum M, Ellingson BM, Tonn JC. Response Assessment in Neuro-Oncology working group and European Association for Neuro-Oncology recommendations for the clinical use of PET imaging in gliomas. Neuro Oncol 2016;18(9):1199-1208.
5. Brugniaux JV, Hodges AN, Hanly PJ, Poulin MJ. Cerebrovascular responses to altitude. Respiratory physiology & neurobiology 2007;158(2-3):212-223.
6. Attwell D, Buchan AM, Charpak S, Lauritzen M, Macvicar BA, Newman EA. Glial and neuronal control of brain blood flow. Nature 2010;468(7321):232-243.
7. Pillai JJ, Mikulis DJ. Cerebrovascular Reactivity Mapping: An Evolving Standard for Clinical Functional Imaging. AJNR American journal of neuroradiology 2015;36(1):7-13.
8. Zaca D, Hua J, Pillai JJ. Cerebrovascular reactivity mapping for brain tumor presurgical planning. World journal of clinical oncology 2011;2(7):289-298.
9. Holodny AI, Schulder M, Liu WC, Maldjian JA, Kalnin AJ. Decreased BOLD functional MR activation of the motor and sensory cortices adjacent to a glioblastoma multiforme: implications for image-guided neurosurgery. AJNR Am J Neuroradiol 1999;20(4):609-612.
10. Hou BL, Bradbury M, Peck KK, Petrovich NM, Gutin PH, Holodny AI. Effect of brain tumor neovasculature defined by rCBV on BOLD fMRI activation volume in the primary motor cortex. NeuroImage 2006;32(2):489-497.
11. Wang Q, Zhang H, Zhang J, Wu C, Zhu W, Li F, Chen X, Xu B. The diagnostic performance of magnetic resonance spectroscopy in differentiating high-from low-grade gliomas: A systematic review and meta-analysis. European radiology 2015.
12. Hsu YY, Chang CN, Jung SM, Lim KE, Huang JC, Fang SY, Liu HL. Blood oxygenation level-dependent MRI of cerebral gliomas during breath holding. Journal of magnetic resonance imaging : JMRI 2004;19(2):160-167.
13. Fierstra J, Sobczyk O, Battisti-Charbonney A, Mandell DM, Poublanc J, Crawley AP, Mikulis DJ, Duffin J, Fisher JA. Measuring cerebrovascular reactivity: what stimulus to use? The Journal of physiology 2013;591(Pt 23):5809-5821.
14. Mutch WA, Mandell DM, Fisher JA, Mikulis DJ, Crawley AP, Pucci O, Duffin J. Approaches to brain stress testing: BOLD magnetic resonance imaging with computer-controlled delivery of carbon dioxide. PloS one 2012;7(11):e47443.

15. Slessarev M, Han J, Mardimae A, Prisman E, Preiss D, Volgyesi G, Ansel C, Duffin J, Fisher JA. Prospective targeting and control of end-tidal CO2 and O2 concentrations. The Journal of physiology 2007;581(Pt 3):1207-1219.
16. Fierstra J, van Niftrik B, Piccirelli M, Burkhardt JK, Pangalu A, Kocian R, Valavanis A, Weller M, Regli L, Bozinov O. Altered intraoperative cerebrovascular reactivity in brain areas of high-grade glioma recurrence. Magnetic resonance imaging 2016;34(6):803-808.
17. Liu WC, Feldman SC, Schulder M, Kalnin AJ, Holodny AI, Zimmerman A, Sinensky R, Rao S. The effect of tumour type and distance on activation in the motor cortex. Neuroradiology 2005;47(11):813-819.
18. Pillai JJ, Zaca D. Comparison of BOLD cerebrovascular reactivity mapping and DSC MR perfusion imaging for prediction of neurovascular uncoupling potential in brain tumors. Technology in cancer research & treatment 2012;11(4):361-374.
19. Pillai JJ, Zaca D. Relative utility for hemispheric lateralization of different clinical fMRI activation tasks within a comprehensive language paradigm battery in brain tumor patients as assessed by both threshold-dependent and threshold-independent analysis methods. NeuroImage 2011;54 Suppl 1:S136-145.
20. Southwell DG, Hervey-Jumper SL, Perry DW, Berger MS. Intraoperative mapping during repeat awake craniotomy reveals the functional plasticity of adult cortex. J Neurosurg 2016;124(5):1460-1469.
21. Chow DS, Horenstein CI, Canoll P, Lignelli A, Hillman EM, Filippi CG, Grinband J. Glioblastoma Induces Vascular Dysregulation in Nonenhancing Peritumoral Regions in Humans. AJR American journal of roentgenology 2016;206(5):1073-1081.
22. Ludemann L, Forschler A, Grieger W, Zimmer C. BOLD signal in the motor cortex shows a correlation with the blood volume of brain tumors. J Magn Reson Imaging 2006;23(4):435-443.
23. Sharma D, Bithal PK, Dash HH, Chouhan RS, Sookplung P, Vavilala MS. Cerebral autoregulation and CO2 reactivity before and after elective supratentorial tumor resection. J Neurosurg Anesthesiol 2010;22(2):132-137.
24. Iranmahboob A, Peck KK, Brennan NP, Karimi S, Fisicaro R, Hou B, Holodny AI. Vascular Reactivity Maps in Patients with Gliomas Using Breath-Holding BOLD fMRI. Journal of neuroimaging : official journal of the American Society of Neuroimaging 2015.
25. Ben Bashat D, Artzi M, Ben Ami H, Aizenstein O, Blumenthal DT, Bokstein F, Corn BW, Ram Z, Kanner AA, Lifschitz-Mercer B, Solar I, Kolatt T, Palmon M, Edrei Y, Abramovitch R. Hemodynamic response imaging: a potential tool for the assessment of angiogenesis in brain tumors. PloS one 2012;7(11):e49416.
26. Sam K, Poublanc J, Sobczyk O, Han JS, Battisti-Charbonney A, Mandell DM, Tymianski M, Crawley AP, Fisher JA, Mikulis DJ. Assessing the effect of unilateral cerebral revascularisation on the vascular reactivity of the non-intervened hemisphere: a retrospective observational study. BMJ open 2015;5(2):e006014.
27. Fierstra J, Conklin J, Krings T, Slessarev M, Han JS, Fisher JA, Terbrugge K, Wallace MC, Tymianski M, Mikulis DJ. Impaired peri-nidal cerebrovascular reserve in seizure patients with brain arteriovenous malformations. Brain : a journal of neurology 2011;134(Pt 1):100-109.
28. Spano VR, Mandell DM, Poublanc J, Sam K, Battisti-Charbonney A, Pucci O, Han JS, Crawley AP, Fisher JA, Mikulis DJ. CO2 blood oxygen level-dependent MR mapping of cerebrovascular reserve in a clinical population, safety, tolerability, and technical feasibility. Radiology 2013;266:592-598.
29. Sobczyk O, Battisti-Charbonney A, Poublanc J, Crawley AP, Sam K, Fierstra J, Mandell DM, Mikulis DJ, Duffin J, Fisher JA. Assessing cerebrovascular reactivity abnormality by comparison to a reference atlas. Journal of cerebral blood flow and metabolism : official journal of the International Society of Cerebral Blood Flow and Metabolism 2014.
30. Fuchtemeier M, Leithner C, Offenhauser N, Foddis M, Kohl-Bareis M, Dirnagl U, Lindauer U, Royl G. Elevating intracranial pressure reverses the decrease in deoxygenated hemoglobin and abolishes the post-stimulus overshoot upon somatosensory activation in rats. Neuroimage 2010;52(2):445-454.
31. Ito S, Mardimae A, Han J, Duffin J, Wells G, Fedorko L, Minkovich L, Katznelson R, Meineri M, Arenovich T, Kessler C, Fisher JA. Non-invasive prospective targeting of arterial P(CO2) in subjects at rest. J Physiol 2008;586(Pt 15):3675-3682.

Figure 1: Illustrative example of cerebrovascular reactivity map and tumor mask

Caption: Axial projected T1-weighted images demonstrating a glioblastoma WHO grade IV in the left frontal region (left upper images, non-contrast and contrast-enhanced T1-weighted images) which was subsequently masked by a staff neuroradiologist (A.P.; lower left image), to determine CVR in that region (far right images). The tumor masked was subsequently flipped in order to determine contralateral CVR in the same region. A separate edema mask was created to specifically measure CVR in that region (the tumor mask was subtracted from the edema mask to determine CVR in the edema region). CVR ranges from normal reactivity (red) to impaired reactivity (yellow-green) to steal phenomenon (blue).

Figure 2: Exemplary cases demonstrating severity of cerebrovascular reactivity impairment

Caption: Axial projected T1-weighted anatomical images and subsequent CVR overlays showing a CVR map of a healthy subject (A), and two patients with diffuse glioma (B & C). Note that the larger tumor lesion (C) exhibits more severely impaired CVR extending over the entire brain. CVR ranges from normal reactivity (red) to impaired reactivity (yellow-green) to steal phenomenon (blue).

Figure 3: Boxplots of CVR findings in healthy subjects and diffuse glioma patients

Box-whisker plots of whole brain CVR, intralesional CVR and CVR measured in perilesional edema (Figure 3A). On the left is whole brain CVR derived from 12 healthy subjects depicted, as a reference. All three aforementioned CVR values (tumor whole brain, intralesional and edema) are significantly lower as compared to the healthy CVR (indicated with * * *; $p<0.01$). CVR intralesional as well as CVR edema are also significantly lower as compared to whole brain tumor CVR ($p<0.05$). Figure 3B shows a significantly lower CVR for the tumor mask as compared to the same masked flipped onto the contralateral hemisphere ($p<0.05$).

Figure 4: Correlation between cerebrovascular reactivity impairment and tumor volume

Caption: Graphic representation of the tumor volume plotted versus degree of CVR impairment for whole brain (A) and intralesional CVR (B). Both analyses showed a significant correlation ($p<0.05$, $R^2= 0.80$ and $p<0.05$, $R^2 = 0.50$, respectively). The dotted red line in Figure 4A indicates normal mean quantitative CVR calculated from the 12 healthy subjects.

Abbreviations: WB = whole brain

Supplementary material

Caption: Supporting Video S1illustrates whole brain normal CVR. Supporting Video S2 illustrates whole brain impaired CVR in a patient with diffuse glioma (specifically a butterfly glioblastoma WHO Grad IV). CVR ranges from normal reactivity (red) to impaired reactivity (yellow-green) to steal phenomenon (blue).

Table 1: Patient and tumor characteristics

Subject	Age	Sex	Histology	WHO Grade	Tumor location	Clinical presentation	CO2 baseline (calibrated)	CO2 Hypercapnia
1	49	F	Oligoastrocytoma	III	right frontal	Epilepsy	39	48
2	39	M	Oligoastrocytoma	III	left frontal	Epilepsy	42	49
3	54	F	Oligoastrocytoma	III	left frontal	Headache, aphasia	41	51
4	32	F	Anaplastic astrocytoma	III	right temporal	Headache	41	51
5	50	M	Oligodendroglioma	III	bifrontal	Headache, Neuropsychological deficits	42	52
6	27	M	Astrocytoma	III	right frontal	Epilepsy	41	50
7	66	M	Glioblastoma	IV	bifrontal	Neuropsychological deficits	38	49
8	81	M	Glioblastoma	IV	left temporal	Aphasia	40	50
9	64	M	Glioblastoma	IV	bifrontal	Headache, Neuropsychological deficits	40	51
10	64	F	Glioblastoma	IV	left parieto-occip	Epilepsy, hemianopsia	40	50
11	91	M	Glioblastoma	IV	right temporal	Headache, vertigo	40	50
12	78	M	Glioblastoma	IV	left frontal	Psychomotoric deficits	40	50

Table 2: CVR findings and tumor volume

	CVR (% BOLD signal change/ mmHg CO_2)				
Subject	**Whole brain**	**Affected hemisphere**	**Unaffected hemisphere**	**intralesional**	**Volume (cm3)**
1	**0.17**	**0.16**	**0.18**	**0.04**	**47.06**
2	**0.22**	**0.22**	**0.22**	**0.17**	**14.76**
3	**0.17**	**0.13**	**0.17**	**0.02**	**7.79**
4	**0.23**	**0.23**	**0.25**	**0.06**	**2.62**
5	**-0.08**	**-0.09**	**-0.05**	**-0.06**	**144.69**
6	**-0.01**	**-0.02**	**0.03**	**-0.07**	**51.76**
7	**0.01**	**-0.01**	**0.02**	**-0.04**	**119.4**
8	**0.1**	**0.1**	**0.08**	**0.02**	**17.6**
9	**0.18**	**0.1**	**0.14**	**0.03**	**43**
10	**0.2**	**0.16**	**0.23**	**0.12**	**28.55**
11	**0.13**	**0.11**	**0.14**	**0.05**	**77.22**
12	**0.04**	**0.09**	**0.1**	**0.01**	**40.44**
Mean(± SD)	**0.11 (0.10)**	**0.10 (0.10)**	**0.13 (0.09)**	**0.03 (0.07)**	**49.57 (0.16)**

Title: Diffuse gliomas exhibit whole brain impaired cerebrovascular reactivity

Running Title: Diffuse gliomas exhibit impaired CVR

Authors: Jorn Fierstra, MD PhD[1]; Christiaan van Niftrik, MD[1]; Marco Piccirelli, PhD[2]; Oliver Bozinov, MD[1]; Athina Pangalu, MD[2]; Niklaus Krayenbühl, MD[1]; Antonios Valavanis, MD[2]; Michael Weller, MD[3]; Luca Regli MD[1]

Affiliations: Departments of Neurosurgery[1], Neuroradiology[2], and Neurology[3], Clinical Neuroscience Center, University Hospital Zurich, University of Zurich, Switzerland

Corresponding author

Jorn Fierstra, MD PhD

Department of Neurosurgery, University Hospital Zurich

Frauenklinikstrasse 10, 8091 Zurich, Switzerland

Phone: +41-44-2551111, Fax: +41-44-2554505 E-mail: jorn.fierstra@usz.ch

Keywords: fMRI, BOLD, diffuse glioma, cerebrovascular reactivity, carbon dioxide

Abstract

Purpose: Cerebral diffuse gliomas exhibit perilesional impaired cerebrovascular reactivity (CVR), yet the degree of impairment as well as its full spatial extent in the brain remains unknown. With quantitative fMRI, we studied twelve subjects with untreated brain diffuse glioma and twelve healthy controls to assess CVR impairment and determine its distribution throughout the brain.

Methods: In a prospective case-control study, quantitative CVR measurements were derived from BOLD fMRI volumes during standardized iso-oxic changes in carbon dioxide. Whole brain CVR was assessed with additional detailed analyses using specific tumor and tissue masks and compared to datasets of healthy controls.

Results: Whole brain CVR was significantly impaired compared to healthy controls (0.11±0.10 versus 0.28±0.8, $p<0.01$). All diffuse glioma patients exhibited even more severely impaired intralesional CVR (mean 0.01±0.06). Increasing tumor volume significantly correlated with severity of intralesional CVR impairment ($p<0.05$, $R^2 = 0.38$), and whole brain CVR impairment ($p<0.05$, $R^2= 0.55$).

Conclusion: Patients with brain diffuse glioma exhibit intralesional and whole brain impaired CVR with severity correlating to tumor volume. Quantitative fMRI may be entertained to study antitumor therapy efficacy by tracking CVR changes and may have a complementary role to better interpret BOLD associated neurovascular uncoupling.

1. Introduction

Neuroimaging plays a pivotal role in treatment response evaluation of brain diffuse gliomas, but is currently limited in accurate depiction of tumor morphology and pathophysiology. (1) (2) For instance, contrast enhanced T1-weighted Magnetic Resonance Imaging (CE-MRI) is imperfect in identifying true tumor tissue due to heterogeneous contrast enhancement, (3) and cannot assess functional parameters such as tumor hemodynamics and molecular characteristics. O-(2-[18F]fluoroethyl)-L tyrosine Positron Emission Tomography (FET-PET) may potentially provide the best functional imaging information, but heterogeneity in (peri)tumor metabolism and long acquisition times may limit clinical applicability. (4) This indicates that the complex molecular biology and pathophysiology of brain diffuse glioma significantly challenges imaging reliability.

From a hemodynamic perspective, diffuse gliomas are believed to disrupt perivascular organization due to co-option of tumor cells accumulating around existing vasculature. (5) As a result the blood vessel walls are destabilized with decreased pericyte coverage, cells thought to be involved in blood flow autoregulation, (6) leading to inability of viable neurons to enhance regional cerebral blood flow (termed `neurovascular uncoupling`) (7-10) a phenomenon that may be more pronounced with increasing tumor volume. (11) Assessing these alterations of cerebrovascular autoregulation with Blood Oxygen-Level Dependent (BOLD) functional (f)MRI cerebrovascular reactivity (CVR) may therefore better depict glioma tissue and locate areas of neurovascular uncoupling and tumor-induced neuroplasticity, ie. healthy brain tissue with `silenced` viable neurons.(7-9,12) This may otherwise manifest itself as false negative activation on conventional task-based BOLD fMRI. Our aim therefore was to elaborate on these encouraging first results by others by further studying the severity of CVR impairment and its distribution throughout the brain.

We prospectively enrolled twelve consecutive subjects harboring untreated brain diffuse glioma, and hypothesized that these patients exhibit widespread impaired CVR extending the contrast enhancing glioma lesion on T1-weighted MRI. Quantitative CVR was derived from a novel standardized BOLD fMRI + CO_2 examination (13,14) and compared to matched healthy controls undergoing the same protocol. In this study, CVR impairment was present over the entire brain in subjects with diffuse glioma.

2. Methods

The study was approved by the cantonal ethics board of the Canton of Zurich, Switzerland (research protocol KEK-ZH-Nr. 2012-0427). Twelve consecutive subjects with newly diagnosed and untreated brain diffuse glioma (defined as either WHO Grade III or Grade IV as confirmed by histopathological diagnosis) as well as twelve age and sex matched healthy controls were prospectively enrolled. Exclusion criteria were the presence of severe cardiopulmonary disease, standard MRI contraindications, age<18 years old, or the inability or refusal to sign informed consent. Furthermore, healthy controls were screened for no medication use, no medical history of neurological disease.

2.1 MRI protocol

Studies were acquired on a 3 Tesla Skyra VD13 (Siemens, Erlangen, Germany) using a 32-channel head coil with the following parameters: an axial 2D EPI BOLD fMRI sequence planned on the ACPC line plus 20° on a sagittal image with voxel size: 3×3×3 mm^3, acquisition of matrix 64x64x35 slices with ascending interleaved acquisition, slice gap 0.3 mm, GRAPPA factor 2 with 32 ref. lines, Repetition Time (TR)/TE 2000/30 ms, flip angle 85°, bandwidth 2368 Hz/Px, Field of View 192x192 mm^2. Secondly, a high resolution 3D T1-weighted anatomical image was acquired with the same orientation as the fMRI scan for co-registration and overlay purposes. The acquisition parameters were: voxel size: 0.8×0.8×1.0

mm^3 with a Field of View 230x230 mm^2 and resolution of 288x288. 176 slices per slab with a thickness of 1 mm, TR/TE 2200/5.14 ms, TI 900 ms, flip angle 8°. The FLAIR images were acquired with the same orientation as the BOLD and T1-weighted images. The acquisition parameters were as followed 0.9x0.9x1.0 mm^3 with a Field of View 230x230 mm^2 and resolution of 256x256, 176 slices per slab with a thickness of 1 mm, TR/TE 4000/387 ms, TI 1800 ms.

2.2 Standardized iso-oxic CO_2 stimulus

All subjects were asked to refrain from caffeine at least 6 hours before scanning. With the use of a custom built computer controlled gas blender (RepirAct™, Thornhill Research Institute, Toronto, Canada) using the prospective gas targeting algorithms of Slessarev et al. (15), to precisely control partial pressure of end-tidal O_2 ($P_{ET}O_2$) and CO_2 ($P_{ET}CO_2$). Specific improvements and novelties of this technique as compared to other vasoactive stimuli have been described in greater detail previously. (13) BOLD signal changes were induced by a single hypercapnia pseudo square wave. The pseudo square wave consisted of a hypercapnia plateau of 50 mmHg CO_2 for 80 seconds following a 100 seconds baseline of 40 mmHg CO_2. Thereafter, a second baseline of 40 mmHg was maintained for another 100 seconds. During the entire protocol iso-oxia (PO_2 100 mmHg) was maintained.

Field Code Changed

Field Code Changed

2.3 Data analysis of BOLD fMRI and T1-weighted image

All images were preprocessed using Statistical Parameter Mapping software (SPM 12, Wellcome Trust Centre for Neuroimaging, Institute of Neurology, University College London; http://www.fil.ion.ucl.ac.uk/spm/). Slice timing correction was applied to correct for the interleaved acquisition. The intra fMRI motion was determined and taken out by realigning the BOLD images to a mean BOLD volume. Subjects with more than 4mm motion were discarded. The T1-weighted image was linearly registered to the mean BOLD volume

for optimal alignment. Automated segmentation of the T1-weighted image yielded grey and white matter, cerebrospinal fluid, skull and skin probability maps. The BOLD images were spatially smoothed with an 8x8x8-mm^3 full width half maximum Gaussian kernel. Temporal smoothing included a low pass filter of 0.125Hz and robust Loess smoothing (dynamic local regression of 6%).

2.4 Cerebrovascular reactivity maps

MRI volumes were analyzed using MATLAB2013 based (The MathWorks, Inc., Natick, United States; (www.matworks.com) in-house written scripts. We determined the optimal delay on a voxel-wise basis by applying an iterative analysis to the data to determine the correct voxel-wise temporal $P_{ET}CO_2$ shift to match the start of the hypercapnia induced BOLD signal change. The shifted $P_{ET}CO_2$ time series was regressed using a linear least square fitting to the BOLD time series on a voxel-per-voxel basis. More details are provided in a previous publication by our group. (16) CVR was defined as the %BOLD signal change per mmHg CO_2. ~~(16)~~ CVR was color-coded between -0.6 and 0.6 and overlaid on the T1 weighted image. Only voxels passing a combined grey and white matter probability of 0.9 were included for overlay and further analysis (Figure 1). Hemispheres were manually segmented in left and right hemisphere and CVR was calculated separately for both.

Formatted: Justified

2.5 Tumor and edema mask determination

The tumor mask was determined by a senior staff neuroradiologist (A.P.). Here, the mask was determined from a contrast enhanced T1-weighted anatomical volume where the contrast-enhancing lesion was depicted. This mask was used to determine intralesional CVR and tumor volume. Intralesional CVR was calculated by projecting the tumor mask on the CVR map (Figure 1). This tumor mask was also mirrored onto the 'unaffected' contralateral hemisphere (excluding the gliomas with a "butterfly" configuration, n= 8) for subsequent

CVR comparison. Regarding this mask only voxels within the grey and white matter were considered for further analysis. Extent of edema was determined and masked using a high resolution FLAIR T2 weighted image. Tumor volume was based on MR voxel proportions and number of voxels within the tumor and calculated in mm^3.

2.6 Statistical Analysis

Continuous variables are presented as mean ± standard deviation. Demographic data and CVR were compared between two groups (diffuse glioma patients versus healthy controls) using independent sample t-tests and Fisher's Exact test [$p<0.05$ was considered significant; $t(24) = 2.064$]. Comparison between the ipsilateral and contralateral tumor masks were done using a paired sample T Test.

As a sub-analysis mean CVR of subjects with grade III and grade IV were compared. Comparisons between groups were done using the Chi-square test or the Fisher's exact test, where appropriate. To corroborate the results of bivariate testing, we constructed a generalized linear model with tumor volume as the independent variable.

3. Results

3.1 Potential confounders affecting CVR measurements in the study cohort

We assessed several comorbidities that could potentially affect CVR findings, such as diabetes, smoking, chronic obstructive pulmonary disease, asthma, hypercholesteremia and hypertension. These did not reveal significant differences in CVR readings between patients with diffuse glioma and healthy controls ($p= 0.45$). Furthermore, since target $P_{ET}CO_2$ and $P_{ET}O_2$ were controlled no significant differences between patients and controls were found for baseline conditions (40.3±1.3 versus 40.5±1.3, $p= 0.55$, respectively), hypercapnia (50 ± 1.4

versus 48.2±1.2, p= 0.43 respectively) and CO_2 step change (p= 0.48). End tidal PCO_2 ($P_{ET}CO_2$) and PO_2 ($P_{ET}O_2$) values for patients are shown in Table 1.

3.2 CVR findings in patients with diffuse glioma and healthy references

To examine whether diffuse glioma impacts cerebrovascular reactivity, we analyzed CVR maps of 12 patients with diffuse glioma (mean age 50 years, range 27-81; 4 females) and compared these to CVR maps of 12 age and sex matched healthy controls. More detailed patient and tumor characteristics are shown in Table 1. Differences in CVR were calculated as the percent change in BOLD signal per mmHg change in $P_{ET}CO_2$ (see Methods section). Whole brain CVR of diffuse glioma patients was significantly impaired compared to healthy controls (0.11±0.10 versus 0.28±0.8, $p<0.01$; Figure 2 & Table 2). Additionally, individual CVR measurements of both hemispheres, ipsi- and contralateral, were also significantly impaired as opposed to healthy controls ($p<0.05$). This suggests that diffuse glioma impacts CVR on a widespread scale.

3.3 CVR findings in patients with diffuse glioma

Further detailed analyses were done on diffuse glioma patients. Ipsilateral CVR was significantly more impaired as compared to contralateral CVR (0.10±0.9 vs 0.13±0.9, $p<0.01$). All diffuse glioma patients exhibited intralesional impaired CVR with an overall mean of 0.01±0.06, which was significantly decreased as compared to whole brain CVR ($p<0.05$). By flipping the tumor mask onto the contralateral hemisphere, a mirror CVR comparison was done (0.07±0.06) which confirmed a significant impaired CVR within the tumor ($p<0.05$).

Perifocal edema was determined from a T2-FLAIR volume (see methods) and subsequently analyzed for CVR. This also demonstrated impaired CVR (0.04±0.05), however intralesional CVR was again more impaired ($p<0.05$). A trend in correlation was observed towards more

severe intralesional and whole brain CVR impairment in WHO grade IV gliomas (grade III (n= 6) versus grade IV (n= 6); 0.12±0.13 vs 0.10±0.07 p=0.77 for whole brain CVR; 0.0±0.06 vs 0.03±0.06 p =0.42 for intralesional CVR). Tumor volume was not a confounder in this analysis. This may actually reach statistical significance in a future, larger series of patients. The significantly impaired CVR findings in patients with diffuse glioma are plotted in Figure 3 for visual appreciation, against a reference CVR value derived from the cohort of healthy subjects. In the supplementary files we have added a movie of whole brain CVR in 1) a healthy subject (Supporting Video S1) and 1) a patient with a diffuse glioma (Supporting Video S2).

3.4 Correlation of CVR impairment versus tumor volume

Since all diffuse glioma patients exhibited whole brain and intralesional CVR impairment, for our final analysis, we determined the association of tumor volume with degree of CVR impairment. Here, severity of intralesional CVR impairment was significantly correlated to tumor volume ($p<0.05$, $R^2 = 0.38$, Figure 4). This correlation was even stronger between whole brain CVR and tumor volume ($p<0.05$, $R^2= 0.55$, Figure 4).

4. Discussion

Quantitative CVR obtained with standardized BOLD fMRI + CO_2 highlights extensive impairment in brain diffuse glioma. All 12 glioma patients exhibited whole brain impaired CVR, and to a greater extent intralesional impaired CVR. Interestingly, a trend was observed towards more severe CVR impairment in glioblastoma (WHO grade IV) patients.

Important to mention is that our data confirm previous findings of intralesional CVR impairment, (7,8,12,17) and that we newly demonstrate presence of CVR impairment in the entire brain with severity correlating to tumor volume. This global presence of impaired CVR

warrants current findings of BOLD fMRI associated perilesional neurovascular uncoupling and tumor-induced neuroplasticity in cerebral diffuse gliomas. Pillai et al. (18,19) have already advocated the importance of a complementary BOLD CVR examination to validate perilesional neurovascular uncoupling, ie. to correct for false negative activation on conventional task-based fMRI. Furthermore, even though the presence of tumor-induced neuroplasticity has univocally been proven by itself, detecting such with BOLD fMRI may have to be interpreted with caution as presence of CVR impairment may also lead to false negative BOLD signal changes. For instance, Southwell et al. (20) measured "less functional reorganization" in patients with larger volume diffuse gliomas. Following this observation Wang et al. (11) have shown that neurovascular uncoupling is more pronounced with increasing tumor volume. Both observations confirm that caution must be taken to interpret these data as increasing CVR impairment may partially influence the readout.
Furthermore, these effects may not be limited solely to the perilesional tissue and our current findings underscore the importance of obtaining a quantitative CVR map of the entire brain in order to better validate the presence of BOLD associated neurovascular uncoupling and tumor induced neuroplasticity.

The exact pathophysiological mechanisms causing this vascular dysregulation appear to be complex and remain to be further elucidated. Animal studies in diffuse glioma have indicated smooth muscle vascular tone disruption due to displacement of astrocyte end-feet covering the vascular surface, ie. tumor cell co-option. (5) As a result the blood vessel walls are destabilized with decreased pericyte coverage, cells thought to be involved in CBF autoregulation, (6) leading to inability of viable neurons to enhance regional blood flow. This vascular dysregulation can be a reason for impaired CVR due to altered autoregulation. A second reason may be abnormal neoangiogenesis following increased tumor metabolism, which often results in angioarchitecture lacking smooth muscle cells and vessels therefore are

not able to respond appropriately to a CO_2 stimulus. (21) In this instance, surrounding healthy tissue can still vasodilate (ie. drop vascular resistance) and will redirect blood flow away from the non-responsive abnormal vessels. Indeed, clinical studies have found that a CO_2 stimulus results in redistribution of cerebral blood flow (CBF) from a tumor region with abnormal angiogenesis to a responsive tumor region and surrounding normal tissue, causing a focal steal phenomenon (ie. severely impaired CVR). (12) In contrast, steal phenomenon has not been found in patients harboring low grade gliomas.(12,22) Finally, locally impaired CVR may also be related to mass effect of the tumor on surrounding healthy tissue. The resulting perifocal pressure may alter cerebrovascular autoregulation. Sharma et al. (23) found that CVR impairment was associated with tumor size and midline shift >5mm. Although none of our subjects exhibited acute clinical signs of raised intracranial pressure, mass effect may have indeed contributed to a decreased BOLD signal. This pressure effect can involve the entire brain with increasing tumor volume. In larger tumors, CBF recruitment may exceed the capacity of CVR of the perilesional tissue and therefore impact on the entire brain. The presence of whole brain impaired CVR for such lesions indicates adjustment of healthy blood vessels, ie. dropping vascular resistance in order to compete for adequate blood flow supply.

Subsequently, with a known increased intralesional Oxygen Extraction Fraction (OEF), intralesional CVR should theoretically be higher as compared to the whole brain CVR, as there should be a higher deoxyhemoglobin content present. With an adequate vasodilatory response to a vasodilatory stimulus, the potential wash-out of deoxyhemoglobin is increased leading to a higher CVR. However, our findings show a more severely impaired intralesional CVR, which makes us believe that the vasodilatory capacity has a much larger effect on the BOLD signal intralesional.

Ideally a multimodal MR imaging protocol, including OEF- and CBF measurements, might better explain the underlying pathophysiology.

Formatted: Font: (Default) Times New Roman, 12 pt, English (United
Formatted: Font: (Default) Times New Roman, 12 pt, English (United
Formatted: Font: (Default) Times New Roman, 12 pt, English (United
Formatted: Font: (Default) Times New Roman, 12 pt, English (United
Formatted: Font: (Default) Times New Roman, 12 pt, English (United
Formatted: Font: (Default) Times New Roman, 12 pt, English (United
Formatted: Font: (Default) Times New Roman, 12 pt, English (United
Formatted: Font: (Default) Times New Roman, 12 pt, English (United
Formatted: Font: (Default) Times New Roman, 12 pt, English (United

Lastly, impaired CVR was also found within the perifocal edema. A report by Ludemann et al. (22) showed that the presence of perifocal edema does not influence CVR measurements obtained with BOLD fMRI, but this finding was based on a small cohort and has not been reproduced. Although we believe that edema may have contributed to perilesional CVR impairment, the fact that intralesional CVR was more severely impaired as compared to ~~as well as~~ whole brain CVR ~~were resp. more and equally impaired~~ shows that this effect may not be significant. The true influence of edema on perilesional CVR will have to be further studied with more detailed analyses.

4.1 Obtaining CVR measurements

The major challenge for quantifying CVR is the inherent limitation of applying a standardized (vaso)active stimulus in order to reliably and sensitively detect CVR abnormalities. (13) Most studies therefore determine breath-hold based CVR to assess impaired (peri-)lesional CVR by comparing CVR values to the assumingly healthy contralateral hemisphere. (7,12,21,22,24,25) Our data, however, demonstrate that quantitative CVR measurements also reveal substantially impaired CVR in the contralateral hemisphere. A finding that has been confirmed recently by Sam et al. (26) using the same technique. Therefore, breath-hold based CVR calculations may lead to type II statistical error.

For over ten years, we have been successfully employing standardized prospective CO_2 targeting for our BOLD related CVR studies (27,28) and have implemented the same protocol for this study with improved methodological CVR analysis. (16) This has resulted in a quantitative and sensitive (voxel-wise) whole brain CVR analysis in patients with diffuse gliomas. The use of a `healthy` contralateral hemisphere or ROI may also be argued based on these data, since all of our subjects exhibited impaired CVR contralaterally. Although a relative CVR difference may be calculated from a contralateral hemisphere or ROI, using the term healthy may be erroneous. A comparison against a statistical control atlas containing

data of healthy volunteers may therefore provide a more sensitive and reliable quantitative measure to assess the degree of CVR impairment. (29)

4.2 Limitations

Theoretically, impaired CVR may have been the consequence of a `dampened` BOLD response by CO_2 elevations or raised intracranial pressure (ICP) as a result of tumor mass including perifocal edema. (23,30) Although the CVR findings appear to discriminate between patients with diffuse glioma and healthy controls, possible confounders such as co-morbidities and glioma characteristics, might have influenced CVR readings. Even though these features did not demonstrate a statistically significant effect, these analyses are underpowered to reveal possible statistical differences in our cohort, with a relatively small sample size of 24 subjects. In addition, the effect of age, pulmonary disease and history of chronic cigarette smoking, which may ordinarily increase the arterial to end-tidal gradient in spontaneously breathing subjects, might influence CVR readings. However, Ito et al. (31) have argued that, with computer controlled prospective end-tidal targeting, the gradient will nevertheless, be small, even in the presence of lung disease, over a large range of induced PCO_2 and O_2 pressure.

5. Conclusion

Patients with brain diffuse glioma exhibit intralesional and whole brain impaired CVR with severity correlating to tumor volume. A quantitative whole brain CVR evaluation may have a complementary role to better assess BOLD associated neurovascular uncoupling.

Acknowledgments

We would like to express our gratitude to the Neuro-MRI team of the University Hospital Zurich for their support and coordination. None of the authors report conflicts of interest or

will gain financially from this manuscript. This work was supported with the University of Zurich `Filling-the-Gap 2015` and `Forschungskredit: Postdoc 2016` initiative.

6. Reference list

1. Wen PY, Kesari S. Malignant gliomas in adults. N Engl J Med 2008;359(5):492-507.
2. Huang RY, Neagu MR, Reardon DA, Wen PY. Pitfalls in the neuroimaging of glioblastoma in the era of antiangiogenic and immuno/targeted therapy - detecting illusive disease, defining response. Front Neurol 2015;6:33.
3. Chung C, Metser U, Menard C. Advances in Magnetic Resonance Imaging and Positron Emission Tomography Imaging for Grading and Molecular Characterization of Glioma. Semin Radiat Oncol 2015;25(3):164-171.
4. Albert NL, Weller M, Suchorska B, Galldiks N, Soffietti R, Kim MM, la Fougere C, Pope W, Law I, Arbizu J, Chamberlain MC, Vogelbaum M, Ellingson BM, Tonn JC. Response Assessment in Neuro-Oncology working group and European Association for Neuro-Oncology recommendations for the clinical use of PET imaging in gliomas. Neuro Oncol 2016;18(9):1199-1208.
5. Brugniaux JV, Hodges AN, Hanly PJ, Poulin MJ. Cerebrovascular responses to altitude. Respiratory physiology & neurobiology 2007;158(2-3):212-223.
6. Attwell D, Buchan AM, Charpak S, Lauritzen M, Macvicar BA, Newman EA. Glial and neuronal control of brain blood flow. Nature 2010;468(7321):232-243.
7. Pillai JJ, Mikulis DJ. Cerebrovascular Reactivity Mapping: An Evolving Standard for Clinical Functional Imaging. AJNR American journal of neuroradiology 2015;36(1):7-13.
8. Zaca D, Hua J, Pillai JJ. Cerebrovascular reactivity mapping for brain tumor presurgical planning. World journal of clinical oncology 2011;2(7):289-298.
9. Holodny AI, Schulder M, Liu WC, Maldjian JA, Kalnin AJ. Decreased BOLD functional MR activation of the motor and sensory cortices adjacent to a glioblastoma multiforme: implications for image-guided neurosurgery. AJNR Am J Neuroradiol 1999;20(4):609-612.
10. Hou BL, Bradbury M, Peck KK, Petrovich NM, Gutin PH, Holodny AI. Effect of brain tumor neovasculature defined by rCBV on BOLD fMRI activation volume in the primary motor cortex. NeuroImage 2006;32(2):489-497.
11. Wang Q, Zhang H, Zhang J, Wu C, Zhu W, Li F, Chen X, Xu B. The diagnostic performance of magnetic resonance spectroscopy in differentiating high-from low-grade gliomas: A systematic review and meta-analysis. European radiology 2015.
12. Hsu YY, Chang CN, Jung SM, Lim KE, Huang JC, Fang SY, Liu HL. Blood oxygenation level-dependent MRI of cerebral gliomas during breath holding. Journal of magnetic resonance imaging : JMRI 2004;19(2):160-167.
13. Fierstra J, Sobczyk O, Battisti-Charbonney A, Mandell DM, Poublanc J, Crawley AP, Mikulis DJ, Duffin J, Fisher JA. Measuring cerebrovascular reactivity: what stimulus to use? The Journal of physiology 2013;591(Pt 23):5809-5821.
14. Mutch WA, Mandell DM, Fisher JA, Mikulis DJ, Crawley AP, Pucci O, Duffin J. Approaches to brain stress testing: BOLD magnetic resonance imaging with computer-controlled delivery of carbon dioxide. PloS one 2012;7(11):e47443.

15. Slessarev M, Han J, Mardimae A, Prisman E, Preiss D, Volgyesi G, Ansel C, Duffin J, Fisher JA. Prospective targeting and control of end-tidal CO2 and O2 concentrations. The Journal of physiology 2007;581(Pt 3):1207-1219.
16. Fierstra J, van Niftrik B, Piccirelli M, Burkhardt JK, Pangalu A, Kocian R, Valavanis A, Weller M, Regli L, Bozinov O. Altered intraoperative cerebrovascular reactivity in brain areas of high-grade glioma recurrence. Magnetic resonance imaging 2016;34(6):803-808.
17. Liu WC, Feldman SC, Schulder M, Kalnin AJ, Holodny AI, Zimmerman A, Sinensky R, Rao S. The effect of tumour type and distance on activation in the motor cortex. Neuroradiology 2005;47(11):813-819.
18. Pillai JJ, Zaca D. Comparison of BOLD cerebrovascular reactivity mapping and DSC MR perfusion imaging for prediction of neurovascular uncoupling potential in brain tumors. Technology in cancer research & treatment 2012;11(4):361-374.
19. Pillai JJ, Zaca D. Relative utility for hemispheric lateralization of different clinical fMRI activation tasks within a comprehensive language paradigm battery in brain tumor patients as assessed by both threshold-dependent and threshold-independent analysis methods. NeuroImage 2011;54 Suppl 1:S136-145.
20. Southwell DG, Hervey-Jumper SL, Perry DW, Berger MS. Intraoperative mapping during repeat awake craniotomy reveals the functional plasticity of adult cortex. J Neurosurg 2016;124(5):1460-1469.
21. Chow DS, Horenstein CI, Canoll P, Lignelli A, Hillman EM, Filippi CG, Grinband J. Glioblastoma Induces Vascular Dysregulation in Nonenhancing Peritumoral Regions in Humans. AJR American journal of roentgenology 2016;206(5):1073-1081.
22. Ludemann L, Forschler A, Grieger W, Zimmer C. BOLD signal in the motor cortex shows a correlation with the blood volume of brain tumors. J Magn Reson Imaging 2006;23(4):435-443.
23. Sharma D, Bithal PK, Dash HH, Chouhan RS, Sookplung P, Vavilala MS. Cerebral autoregulation and CO2 reactivity before and after elective supratentorial tumor resection. J Neurosurg Anesthesiol 2010;22(2):132-137.
24. Iranmahboob A, Peck KK, Brennan NP, Karimi S, Fisicaro R, Hou B, Holodny AI. Vascular Reactivity Maps in Patients with Gliomas Using Breath-Holding BOLD fMRI. Journal of neuroimaging : official journal of the American Society of Neuroimaging 2015.
25. Ben Bashat D, Artzi M, Ben Ami H, Aizenstein O, Blumenthal DT, Bokstein F, Corn BW, Ram Z, Kanner AA, Lifschitz-Mercer B, Solar I, Kolatt T, Palmon M, Edrei Y, Abramovitch R. Hemodynamic response imaging: a potential tool for the assessment of angiogenesis in brain tumors. PloS one 2012;7(11):e49416.
26. Sam K, Poublanc J, Sobczyk O, Han JS, Battisti-Charbonney A, Mandell DM, Tymianski M, Crawley AP, Fisher JA, Mikulis DJ. Assessing the effect of unilateral cerebral revascularisation on the vascular reactivity of the non-intervened hemisphere: a retrospective observational study. BMJ open 2015;5(2):e006014.
27. Fierstra J, Conklin J, Krings T, Slessarev M, Han JS, Fisher JA, Terbrugge K, Wallace MC, Tymianski M, Mikulis DJ. Impaired peri-nidal cerebrovascular reserve in seizure patients with brain arteriovenous malformations. Brain : a journal of neurology 2011;134(Pt 1):100-109.
28. Spano VR, Mandell DM, Poublanc J, Sam K, Battisti-Charbonney A, Pucci O, Han JS, Crawley AP, Fisher JA, Mikulis DJ. CO2 blood oxygen level-dependent MR mapping of cerebrovascular reserve in a clinical population, safety, tolerability, and technical feasibility. Radiology 2013;266:592-598.
29. Sobczyk O, Battisti-Charbonney A, Poublanc J, Crawley AP, Sam K, Fierstra J, Mandell DM, Mikulis DJ, Duffin J, Fisher JA. Assessing cerebrovascular reactivity abnormality by comparison to a reference atlas. Journal of cerebral blood flow and metabolism : official journal of the International Society of Cerebral Blood Flow and Metabolism 2014.
30. Fuchtemeier M, Leithner C, Offenhauser N, Foddis M, Kohl-Bareis M, Dirnagl U, Lindauer U, Royl G. Elevating intracranial pressure reverses the decrease in deoxygenated hemoglobin and abolishes the post-stimulus overshoot upon somatosensory activation in rats. Neuroimage 2010;52(2):445-454.
31. Ito S, Mardimae A, Han J, Duffin J, Wells G, Fedorko L, Minkovich L, Katznelson R, Meineri M, Arenovich T, Kessler C, Fisher JA. Non-invasive prospective targeting of arterial P(CO2) in subjects at rest. J Physiol 2008;586(Pt 15):3675-3682.

Figure 1: Illustrative example of cerebrovascular reactivity map and tumor mask

Caption: Axial projected T1-weighted images demonstrating a glioblastoma WHO grade IV in the left frontal region (left upper images, non-contrast and contrast-enhanced T1-weighted images) which was subsequently masked by a staff neuroradiologist (A.P.; lower left image), to determine CVR in that region (far right images). The tumor masked was subsequently flipped in order to determine contralateral CVR in the same region. A separate edema mask was created to specifically measure CVR in that region (the tumor mask was subtracted from the edema mask to determine CVR in the edema region). CVR ranges from normal reactivity (red) to impaired reactivity (yellow-green) to steal phenomenon (blue).

Figure 2: Exemplary cases demonstrating severity of cerebrovascular reactivity impairment

Caption: Axial projected T1-weighted anatomical images and subsequent CVR overlays showing a CVR map of a healthy subject (A), and two patients with diffuse glioma (B & C). Note that the larger tumor lesion (C) exhibits more severely impaired CVR extending over the entire brain. CVR ranges from normal reactivity (red) to impaired reactivity (yellow-green) to steal phenomenon (blue).

Figure 3: Boxplots of CVR findings in healthy subjects and diffuse glioma patients

Box-whisker plots of whole brain CVR, intralesional CVR and CVR measured in perilesional edema (Figure 3A). On the left is whole brain CVR derived from 12 healthy subjects depicted, as a reference. All three aforementioned CVR values (tumor whole brain, intralesional and edema) are significantly lower as compared to the healthy CVR (indicated with * * *; $p<0.01$). CVR intralesional as well as CVR edema are also significantly lower as compared to whole brain tumor CVR ($p<0.05$). Figure 3B shows a significantly lower CVR for the tumor mask as compared to the same masked flipped onto the contralateral hemisphere ($p<0.05$).

Figure 4: Correlation between cerebrovascular reactivity impairment and tumor volume

Caption: Graphic representation of the tumor volume plotted versus degree of CVR impairment for whole brain (A) and intralesional CVR (B). Both analyses showed a significant correlation ($p<0.05$, $R^2= 0.80$ and $p<0.05$, $R^2 = 0.50$, respectively). The dotted red line in Figure 4A indicates normal mean quantitative CVR calculated from the 12 healthy subjects.

Abbreviations: WB = whole brain

Supplementary material

Caption: Supporting Video S1illustrates whole brain normal CVR. Supporting Video S2 illustrates whole brain impaired CVR in a patient with diffuse glioma (specifically a butterfly glioblastoma WHO Grad IV). CVR ranges from normal reactivity (red) to impaired reactivity (yellow-green) to steal phenomenon (blue).

Table 1: Patient and tumor characteristics

Subject	Age	Sex	Histology	WHO Grade	Tumor location	Clinical presentation	CO2 baseline (calibrated)	CO2 Hypercapnia
1	49	F	Oligoastrocytoma	III	right frontal	Epilepsy	39	48
2	39	M	Oligoastrocytoma	III	left frontal	Epilepsy	42	49
3	54	F	Oligoastrocytoma	III	left frontal	Headache, aphasia	41	51
4	32	F	Anaplastic astrocytoma	III	right temporal	Headache	41	51
5	50	M	Oligodendroglioma	III	bifrontal	Headache, Neuropsychological deficits	42	52
6	27	M	Astrocytoma	III	right frontal	Epilepsy	41	50
7	66	M	Glioblastoma	IV	bifrontal	Neuropsychological deficits	38	49
8	81	M	Glioblastoma	IV	left temporal	Aphasia	40	50
9	64	M	Glioblastoma	IV	bifrontal	Headache, Neuropsychological deficits	40	51
10	64	F	Glioblastoma	IV	left parieto-occip	Epilepsy, hemianopsia	40	50
11	91	M	Glioblastoma	IV	right temporal	Headache, vertigo	40	50
12	78	M	Glioblastoma	IV	left frontal	Psychomotoric deficits	40	50

Table 2: CVR findings and tumor volume

	CVR (% BOLD signal change/ mmHg CO_2)				
Subject	**Whole brain**	**Affected hemisphere**	**Unaffected hemisphere**	**intralesional**	**Volume (cm3)**
1	**0.17**	**0.16**	**0.18**	**0.04**	**47.06**
2	**0.22**	**0.22**	**0.22**	**0.17**	**14.76**
3	**0.17**	**0.13**	**0.17**	**0.02**	**7.79**
4	**0.23**	**0.23**	**0.25**	**0.06**	**2.62**
5	**-0.08**	**-0.09**	**-0.05**	**-0.06**	**144.69**
6	**-0.01**	**-0.02**	**0.03**	**-0.07**	**51.76**
7	**0.01**	**-0.01**	**0.02**	**-0.04**	**119.4**
8	**0.1**	**0.1**	**0.08**	**0.02**	**17.6**
9	**0.18**	**0.1**	**0.14**	**0.03**	**43**
10	**0.2**	**0.16**	**0.23**	**0.12**	**28.55**
11	**0.13**	**0.11**	**0.14**	**0.05**	**77.22**
12	**0.04**	**0.09**	**0.1**	**0.01**	**40.44**
Mean(± SD)	**0.11 (0.10)**	**0.10 (0.10)**	**0.13 (0.09)**	**0.03 (0.07)**	**49.57 (0.16)**

Figure 1

Click here to download high resolution image

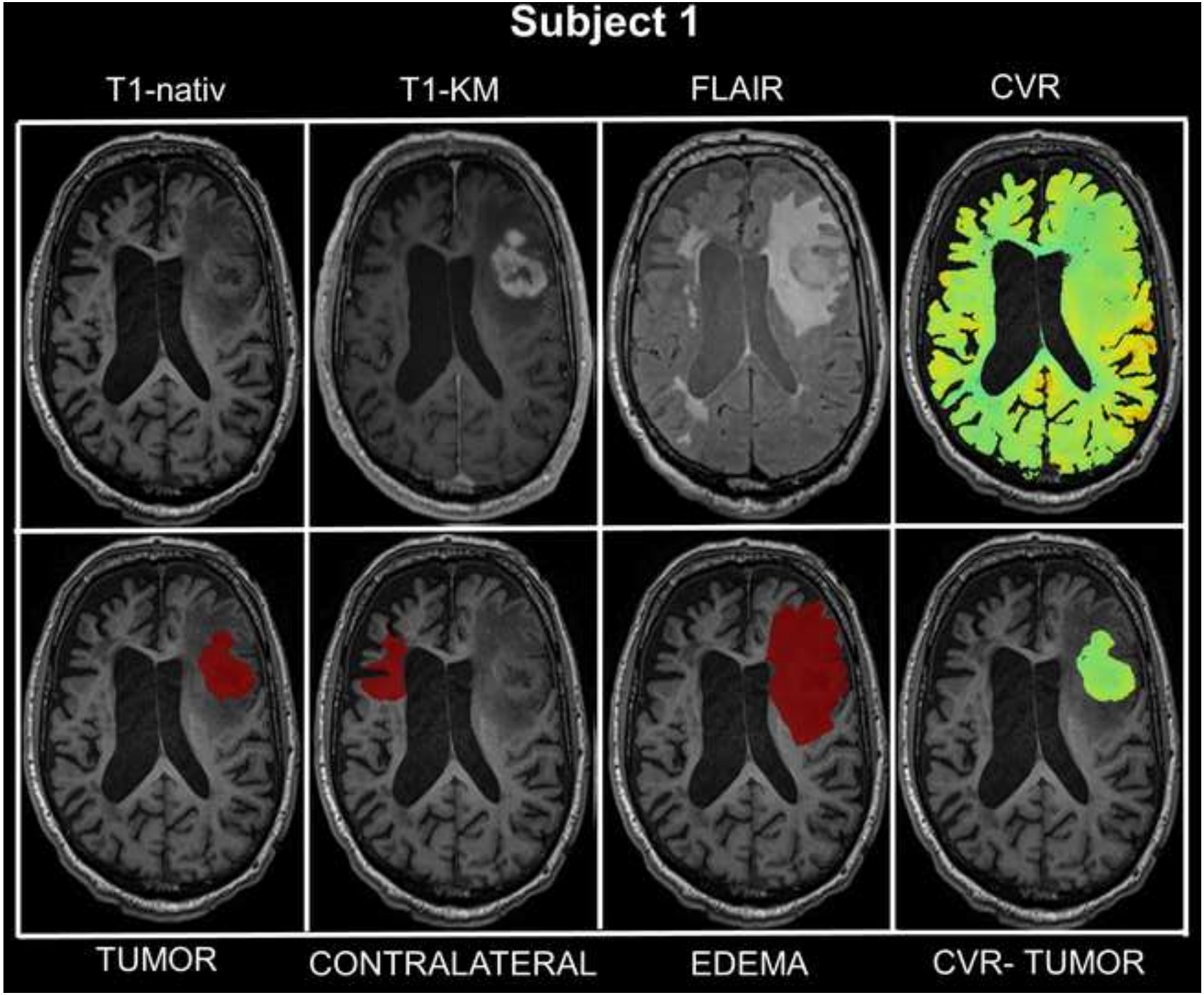

Figure 2

Click here to download high resolution image

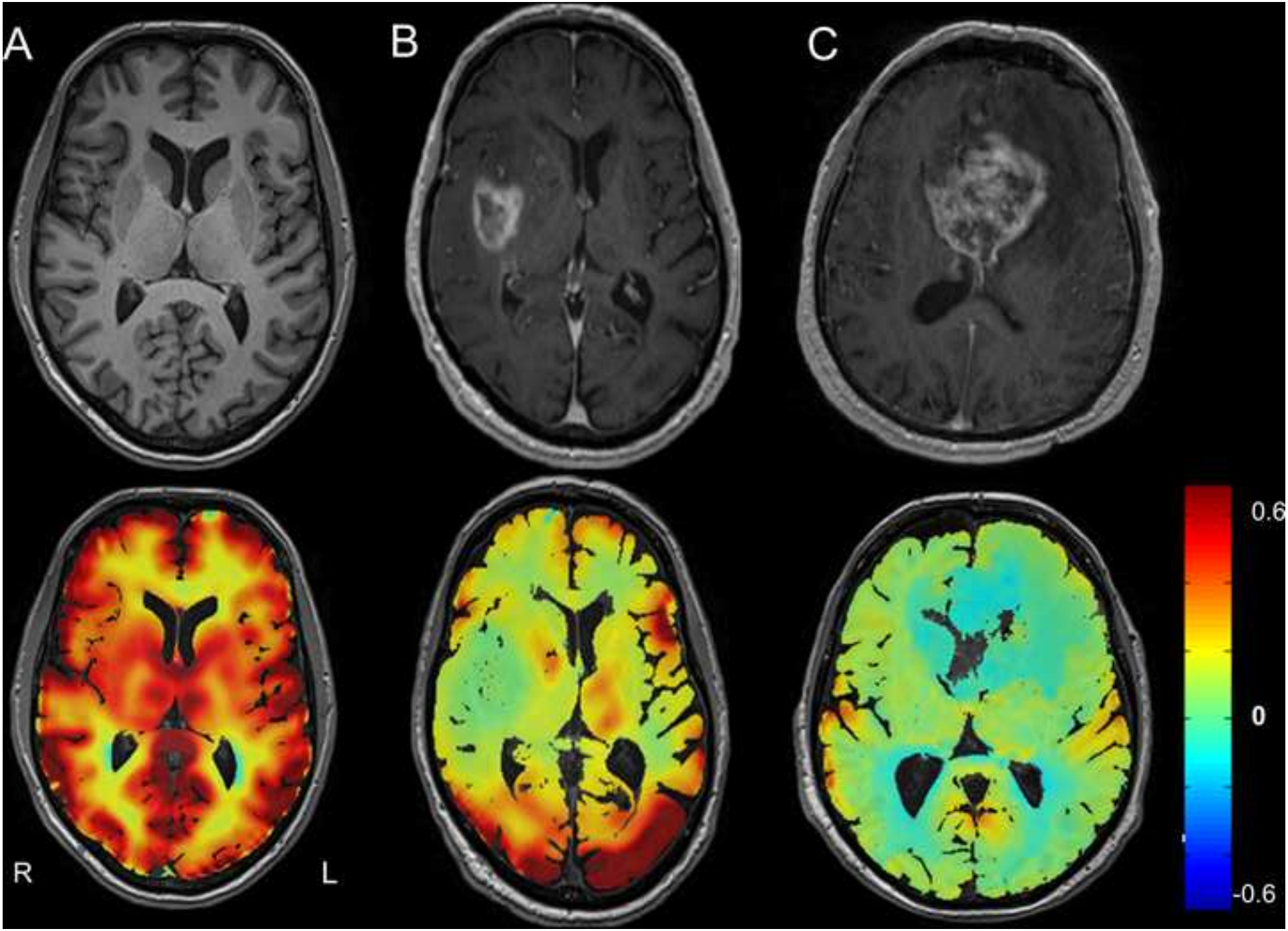

Figure 3
Click here to download high resolution image

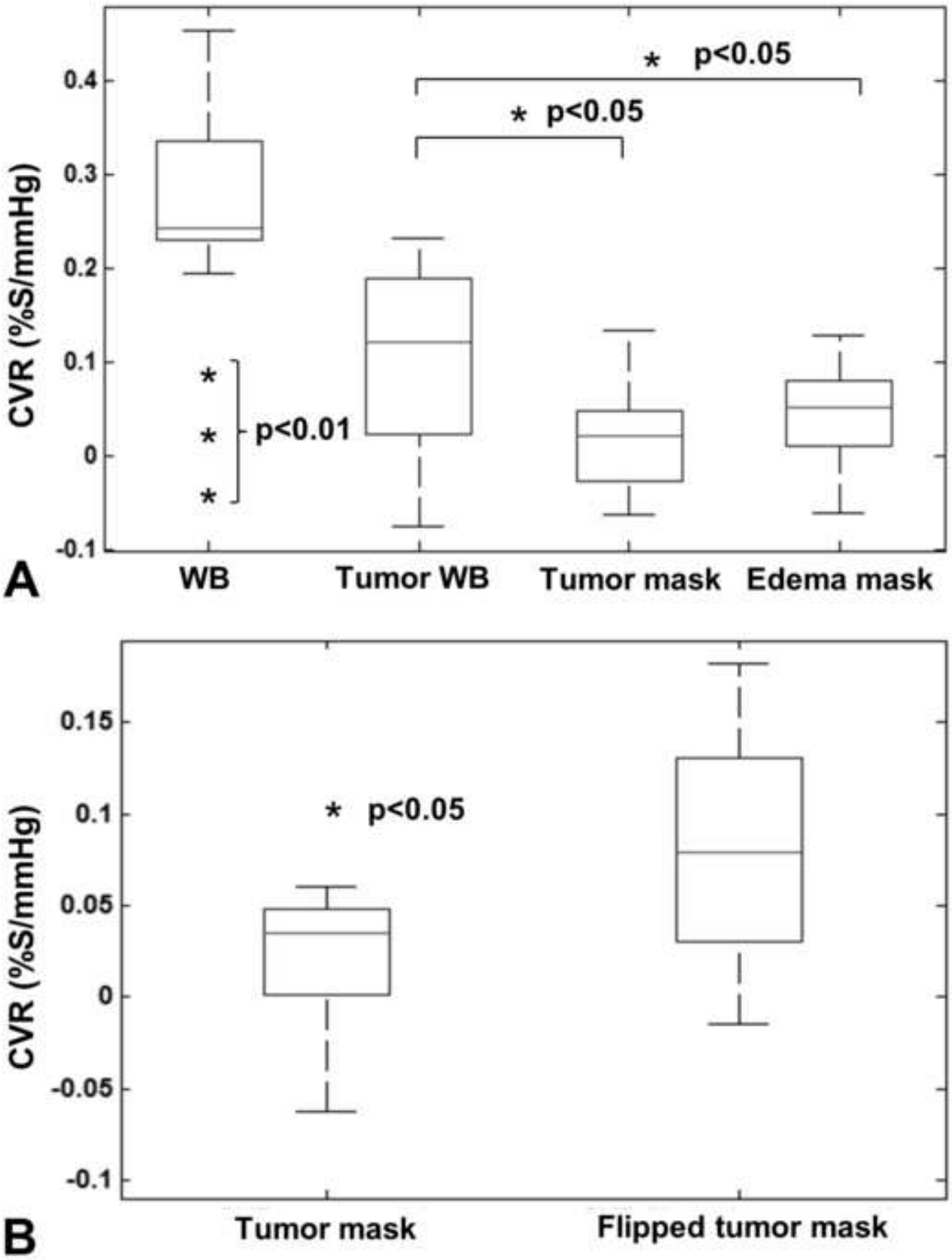

Figure 4

Click here to download high resolution image

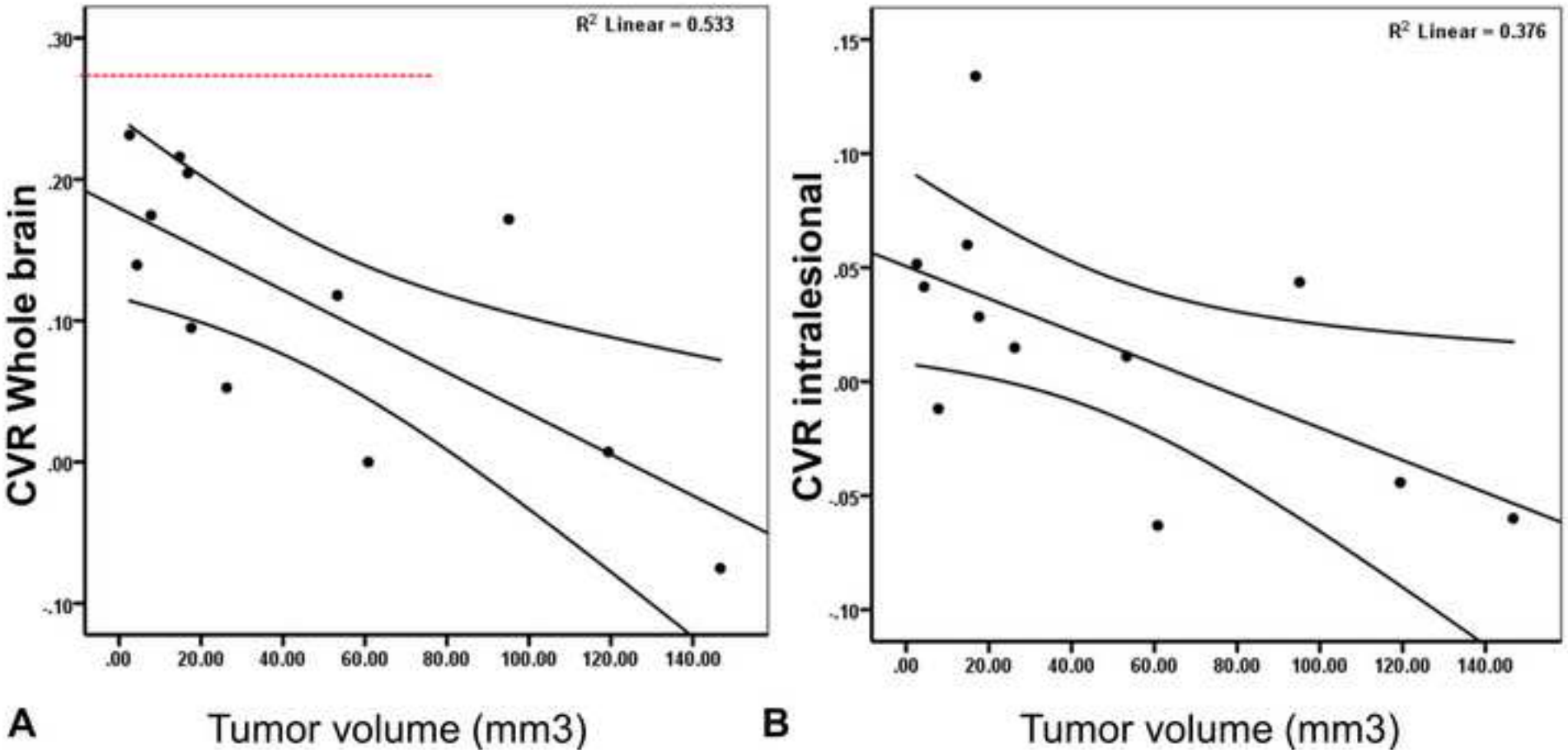

Table 1

Subject	Age	Sex	Histology	WHO Grade	Tumor location	Clinical presentation	CO2 baseline (calibrated)	CO2 Hypercapnia
1	49	F	Oligoastrocytoma	III	right frontal	Epilepsy	39	48
2	39	M	Oligoastrocytoma	III	left frontal	Epilepsy	42	49
3	54	F	Oligoastrocytoma	III	left frontal	Headache, aphasia	41	51
4	32	F	Anaplastic astrocytoma	III	right temporal	Headache	41	51
5	50	M	Oligodendroglioma	III	bifrontal	Headache, Neuropsychological deficits	42	52
6	27	M	Astrocytoma	III	right frontal	Epilepsy	41	50
7	66	M	Glioblastoma	IV	bifrontal	Neuropsychological deficits	38	49
8	81	M	Glioblastoma	IV	left temporal	Aphasia	40	50
9	64	M	Glioblastoma	IV	bifrontal	Headache, Neuropsychological deficits	40	51
10	64	F	Glioblastoma	IV	left parieto-occip	Epilepsy, hemianopsia	40	50
11	91	M	Glioblastoma	IV	right temporal	Headache, vertigo	40	50
12	78	M	Glioblastoma	IV	left frontal	Psychomotoric deficits	40	50

Table 2

	CVR (% BOLD signal change/ mmHg CO_2)				
Subject	**Whole brain**	**Affected hemisphere**	**Unaffected hemisphere**	**intralesional**	**Volume (cm3)**
1	**0.17**	**0.16**	**0.18**	**0.04**	**47.06**
2	**0.22**	**0.22**	**0.22**	**0.17**	**14.76**
3	**0.17**	**0.13**	**0.17**	**0.02**	**7.79**
4	**0.23**	**0.23**	**0.25**	**0.06**	**2.62**
5	**-0.08**	**-0.09**	**-0.05**	**-0.06**	**144.69**
6	**-0.01**	**-0.02**	**0.03**	**-0.07**	**51.76**
7	**0.01**	**-0.01**	**0.02**	**-0.04**	**119.4**
8	**0.1**	**0.1**	**0.08**	**0.02**	**17.6**
9	**0.18**	**0.1**	**0.14**	**0.03**	**43**
10	**0.2**	**0.16**	**0.23**	**0.12**	**28.55**
11	**0.13**	**0.11**	**0.14**	**0.05**	**77.22**
12	**0.04**	**0.09**	**0.1**	**0.01**	**40.44**
Mean(± SD)	**0.11 (0.10)**	**0.10 (0.10)**	**0.13 (0.09)**	**0.03 (0.07)**	**49.57 (0.16)**